RESEARCH ARTICLE

Fabrication of nano S646 bioactive glass and investigation of its addition to chitosan nanocomposites / carbon nanotubes for bone regeneration

Fatemeh Mirjalili[1]*, Mahboobeh Mahmoodi[2,3], Farniya Mohamadifar[2]

[1] Department of Material Engineering, Maybod Branch, Islamic Azad University, Maybod, Iran
[2] Department of Biomedical Engineering, Yazd Branch, Islamic Azad University, Yazd, Iran
[3] Joint Reconstruction Research Center, Tehran University of Medical Sciences, Tehran, Iran

ARTICLE INFO

Article History:
Received 2021-10-24
Accepted 2022-02-22
Published 2022-09-30

Keywords:
Bioglass of S646,
Chitosan,
Carbon nanotube,
MTT assay.

ABSTRACT

Nanoscale bioactive glasses have been gaining attention due to their superior osteoconductivity. The combination of bioactive glass nanoparticles with polymeric systems enables the production of nanocomposites with potential to be used in a series of orthopedic applications, including tissue engineering and regenerative.
This research has been done to study characteristic and biocompatible evaluation of a nano bio composite ceramic. In this regard synthesis of this S646 bioactive glass has been considered afterwards, the bioglass S646/chitosan/ carbon nanotube is synthesized with different amounts of S646 bioactive glass by sol-gel method. The synthesized nanoparticles and nanocomposites are characterized by Field Emission Scanning Electron Microscope, X-ray Powder Diffraction, and Fourier-Transform Infrared Spectroscopy to evaluate crystal structure, microstructure and morphology. The results indicated that, the synthesized bioglass S646/chitosan/carbon nantube nanocomposite has average particle size of about 41-49 nm and percentages of crystallinity about 64-86% for all samples. The result of FT-IR analyses showed the purity in the structure of bioglass of S646 and nano composite.The outcomes revealed that, with increasing the amount of S646 bioactive glass the shape of the particles changed from spherical and the particle size was reduced owing to the increase in amorphous phase in the material which reduced the crystallinity and crystal size of nanocomposite particles. The result of MTT assay indicated nontoxicity and also increasing the percentage of bioactive glass increased cell viability.

How to cite this article
Mirjalili F., Mahmoodi M., Mohamadifar F., Fabrication of nano S646 bioactive glass and investigation of its addition to chitosan nanocomposites / carbon nanotubes for bone regeneration. J. Nanoanalysis., 2022; 9(3): 182-192.
DOI: 10.22034/jna.2022.1943284.1275

INTRODUCTION

Bone regeneration is a complex cascade of biological events controlled by numerous molecules that affords signals at local injury sites allowing progenitors and inflammatory cells to transfer and generate healing processes. Conventional tissue engineering strategies use combination of cells, biodegradable scaffolds and systemic administration of bioactive molecules to support natural routes of tissue regeneration and development [1-3]. Several approaches for controlled biomolecule delivery from scaffolds have been established in bone tissue engineering. One of the most common methods to complete control and localized release of biomolecules is to combine them within biomaterials during the phase of scaffold fabrication [4].

Bone is a special connective tissue that supplies structural funding for the body organs and is an emergency reservoir of calcium in the alteration phase because of a disease, or some pathological

* Corresponding Author Email: *fm.mirjalili@gmail.com*

processes through life [1, 2]. Bio-ceramic is one of the serious substitutes for renewing bone weakness, which may either have the role of providing maintenance, filling hollow spaces or improving the biological action of in situ bone tissue [3, 4]. The inherent characteristics such as biocompatibility, bioinert and durability of these materials permit them to act as a chief selection in engineering orthopedic or orthodontic implants [2, 5]. Bio-ceramics are necessary separations of biomaterials, which are employed in a variability of clinical applications, including dental materials, spinal cord repair, orthopedic applications, and drug delivery in the form of powder, coating, and bulk [5-7]. Contrary to metal alloys, there are known biocompatible ceramics and glasses with outstanding biological properties that generate a strong chemical bond with tissue in a short time[6] and display the appropriate biological answer in the junction of bone and tissue and thus have widespread applications in medicine [7,8]. However, due to their unsuitable physical properties, their demand is challenged with problems in sections under mechanical load [9]. However, there are some problems of these approaches which limit their extensive usage, such as prolonged surgical time and supporter site morbidity for auto graft and adverse immune comeback and pathogen disease transmission for allograft. These difficulties have directed researchers to the growth of bone substitute materials [8–10].Chemically, chitosan is a linear amino polysaccharide, composed of glucosamine and N-acetyl glucosamine units linked by b (1–4) glycosidic bonds formed by N-deacetylation of chitin (its parent polymer). Chitin, the second most abundant biopolymer is mostly found in exoskeletons of crustaceans and cell walls of fungi [11].Chitosan is a polycationic polymer featuring free acetamide groups and hydroxyl functions linked to the glucopyranose rings that are susceptible to react through nucleophilic attack [12]. A wide range of chitosan functionalization can be achieved through selective modification of the free amino groups [13,14]. According to the chemical carcinogenesis research information system [15], chitosan has no mutagenic results, which creates it a nominee for biomedical application. Chitosan is a biodegradable, biocompatible and bio adhesive polysaccharide. It has been shown to be soft tissue compatible and non-toxic in usable concentrations and widely used in pharmaceutical research and in industry as a transporter for drug delivery and as biomedical material [12].

The first reported bioactive glass (BG) was formed by Professor Larry Hench in 1969 with the composition of 45 wt.% SiO_2, 24.5 wt.% Na_2O, 24.5 wt.% CaO and 6 wt.% P_2O_5 (Cooper 2006). This discovery was also the beginning of the second generation of biomaterials that had the ability to bond with host tissues [4, 16]. The most amazing feature about the BG was finding the ability to development very strong interfacial bonds with adjoining tissues. Moreover, BG has the highest bioactivity in vivo index (IB>8) among all bio ceramics [6, 17].

In spite of its astounding biocompatibility and bone bonding capability, BG has limited demands as a scaffold material due to its poor mechanical properties [7,9].The most amazing feature about the BG finding was its ability to improve very strong interfacial bonds with surrounding tissues [10]. Moreover, BG has the highest *in vivo* bioactivity index among all bio ceramics [6]. In spite of its surprising biocompatibility and the bone bonding capability, BG has limited requests as a scaffold material due to its poor mechanical properties [7, 10]. The mixture of the bioactive glass particles with chitosan affords its special properties such as augmentation of bioactivity and mechanical properties. The carbon nanotube (CNTs) is one type of nanomaterials with potential tissue engineering (TE) applications [6,18]. It has been used for the regeneration of different tissues including bone and cartilage [19-21]. However, the insufficient porosity and toughness are known as their important drawbacks for tissue engineering applications which are necessary for vascularization and cellular ingrowth [22] and load-bearing circumstances [23, 24], respectively. The carbon nanotube has been used as a supplementary component owing to its unique mechanical and bioactivity properties [25,26]. Nevertheless, when using CNTs as a second component in either ceramic, polymer or metal composite, the distribution of carbon nanotube and carbon nanotube/matrix interaction factor is a serious issue because the uniform dispersion leads to real load transfer to the nanotube system and has an effect on the properties of the final composite [18, 27]. The other significant factor is wettability of CNTs [19,28] because they are intrinsically highly hydrophobic and chemically inert in nature which may compromise the effectiveness of CNTs-matrix interactions. Thus, surface modification (e.g. using surfactant) is suggested to achieve effective CNTs-

matrix interaction [29-31].

Serg et al in 2020 investigated on the review of bioactive glass/natural polymer composites.This review presented the state of the art and upcoming perspectives of collagen, gelatin, silk fibroin, hyaluronic acid, chitosan, alginate, and cellulose matrices combined with BG particles to improve composites such as scaffolds, injectable fillers, membranes, hydrogels, and coatings. Highlighting is dedicated to the biological potentialities of these hybrid systems, which stared rather promising toward a wide spectrum of requests [32]. Moreover, Shrestha et al.,reported the Engineered cellular microenvironments from functionalized multiwalled carbon nanotubes integrating Zein/ Chitosan @Polyurethane for bone cell regeneration. They enhanced functional connectivity between cells and scaffolds. Also, Zein/Chitosan and fMWCNTs have synergistic effects to support osteogenic differentiation [33].

To our best knowledge, the CNT-reinforced bioglass S646/chitosan containing various amounts of s646 bioactive glass has not been reported in the literature. To this end, the novelty of this report is to prepare the bioactive glass S646 and then preparation of bio glass S646/chitosan CNTs nano composite via adding different amounts of bio glass S646 as the second phase. Then, the morphological and microstructure properties and cell viability of nano composites are being investigated.

EXPERIMENTAL ACTIVITIES

Synthesis of bioactive glass of S646 and bioactive glasses of S646/ chitosan/CNT nanocomposites

For synthesis of bioactive glasses of S646/ chitosan/CNT nanocomposites, two sols of bioactive glass and chitosan were prepared. The sol of bioactive glass of S646 was prepared by hydrolysis of 56 ml tetraethoxysilane (TEOS,98%,Merck) in 350 ml of the distilled water and 350 ml ethanol (98%, Merck) at room temperature and then the pH adjusted at 2 by nitric acid (96%, Merck) with continuous stirring for 1 h. Then, 24.5 g hydrated calcium nitrate (97%, Merck) was added to the above solution and continued the stirring until the dissolving. After that, 21.07 g $NaNO_3$ (97%, Merck) was added to the above mixture (the previous mixture was named solution A) and then, 10 g ethylene glycol(99%, Merck) and 3.43 g ammonium dehydrogenase phosphate were added to 400 ml the distilled water (this mixture was named solution B). Furthermore, solution (B) was gradually added to solution (A) with continuous stirring overnight. The obtained sol was dried at 60°C temperature for 12 h until it became uniform and transparent gel. The obtained gels were centrifuged and washed with ethanol four times and then dried at 100 °C for 48 h, and subsequently grinded with mortar and pestle.

CNTs prepared by the Chengdu Institute of Organic Chemistry, Chinese Academy of Sciences. The suspensions of 0.05 g chitosan with 100 ml of acetic acid 3% were mixed and vigorously stirred at 25°C for 30 min. After that 0.0005 g CNT was slowly added to the solution and stirred until it became uniform. Then, different amounts of S646 bioactive glass (0.0045, 0.0075, 0.01 g) were vigorously added to the solution and stirred at 25°C for 12 h and dried at 100 °C for 48 h.To study and evaluate the thermal behavior of a S646 bioactive glass powder and to estimate the calcination temperature as well as the crystallinity and the simulated particle size of S646 glass, the simultaneous thermal analysis (STA,) NETZSCH STA 449 F1, Germany) was performed. Phase identification was carried out by X-ray diffraction (XRD, PW1800, Philips) using nickel-filtered Cu Kα radiation in the range of 2θ = 10°-80° with a scanning speed of 5° min^{-1}.The crystallite size was determined by the Scherrer method. The equation was calculated as below:

$$t = 0.89\lambda/\beta\cos\theta \quad (1)$$

Where t is the crystallite size (in nm), λ is the wavelength of X-ray diffraction (in nm), β is the full width at half-maximum, and θ is the Bragg diffraction angle. (Lindfors 2010; Kolk 2012).The crystallinity degree of the hydroxyapatite phase was calculated using X-ray diffraction patterns according to equation 2:

$$X_c = 1-(V_{112/300}-I_{300}) \quad (2)$$

Where, X_c is the degree of crystallinity of the powder and $V_{112/300}$ is the intensity of the cavity between the diffraction peaks (112) and (300) [34, 35].

Fourier transform infrared spectroscopy (FT-IR, Perkin Elmer Spectrum 100) was conducted by the universal attenuated total reflection (UATR) method. Microstructures and morphology of powders were identified by transmission electron microscopy (Philips-Zeiss) and scanning electron microscopy (SEM, PHENOM).

Cell proliferation and viability analysis

In the next step, the proliferation and survival

of L929 cells on the surface of the samples were evaluated by MTT assay. To prepare the samples, a common protocol for this test was used. In this way, 5 mg of each of the samples was mixed in the medium and incubated at 37 ° C for 72 h. These samples were filtered to prevent contamination. After extracting the cells desired in the culture plate, the number of wells were considered as controls and some were considered as the test samples. After the desired time, the culture medium was discarded and a certain volume of solution was spilled on the cells and then, the cells were incubated in this solution. At this time, the MTT ring was broken, breaking the ring created crystalline purple color. The amount of this color was directly related to the living cells. Next, the supernatant was discarded and the cells were washed. At the end, the absorbance of the solution was calculated by the spectrophotometer.

The following formula was then used to determine the survival rate:

$$\text{Cell Viability\%} = \frac{ODs}{ODc}$$

ODs and ODc are optical density sample and optical density control, respectively.

Statistical analysis

Experiments were performed in three replications, and the results were reported as the average ± standard deviation. The statistical study of the quantitative data was performed using one-way ANOVA analysis.

RESULTS AND DISCUSSIONz

Thermal analysis (STA) of S646 bioactive glass

The results of the TG / DTA test performed on a S646 dry gel (before stabilization or calcination) in the range of 25-1000 ° C designated a few occurrences (Fig. 1). In the temperature range of 25- 200 ℃, an endothermic reaction was ensued which related to the exit of moisture and the liquids in the dry gel. At temperatures of 200-645 ℃, several endothermic and exothermic reactions were recognized to the degradation of organic elements such as silanol groups or the onset of nitrate decomposition reactions [7]. The thermal decomposition of nitrates was a phase reaction that, happened thermodynamically at temperatures below 550 ° C. The major part of organic detoxification and consequent weight loss occurred at 545-645 ℃.With regard to the TGA curve, after the thermal decomposition of the nitrates, the mass changes in the specimens became constant and stable. Then, an exothermic peak was observed at temperature of about 800 ℃ which can be attributed to the crystallization process of the glass [7,16]. The weight variation curve with temperature can be divided into three regions which are shown in Table 1.

One of the steps to be taken into account in the bioactive action of bioactive glass was the formation of Si-OH groups of surface that were actually apatite germination sites [1]. Also, the sol-gel synthesized glass integrally contained hydroxyl groups in its own network. At around 645 ° C, almost all nitrates were removed from the glass network. Therefore, the temperature of 655 ℃ was chosen as the appropriate stabilization temperature for the biologically active glass. The selection of high temperatures led to glass crystallization and thus the production of ceramic glass.

Fig. (2) shows the XRD patterns of the S646 bioactive glass. Based on the X-ray diffraction pattern, it represented a broad shorter form that expressed the amorphous structure of the nano powder synthesized. Although, the high degree of amorphous was detectable from this pattern, the peaks belonged to the crystalline phases were visible at an angle of 22 ° C that was related to the effects of crystalline phases of silicate (JCPDS 85033).

X-ray diffraction pattern of chitosan /carbon nanotube composite samples is shown in Fig. 3.

It was understood that all the peaks identified in the diffraction pattern were related to the structure of nano tube carbon (CNT, JCPDS No. 06-0696)

Table 1: The weight loss of gel with increasing temperature.

Weight loss			
Stage 3 800-1000 ℃	Stage 2 200-700 ℃	Stage 1 25-200 ℃	Sample
1.5%	37.3%	1.2%	BG-100%

a. X-ray diffraction analysis:

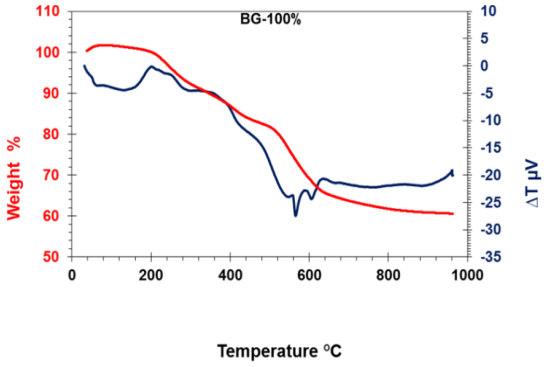

Fig. 1: TG-DTA thermo gram of S646 bioactive glass

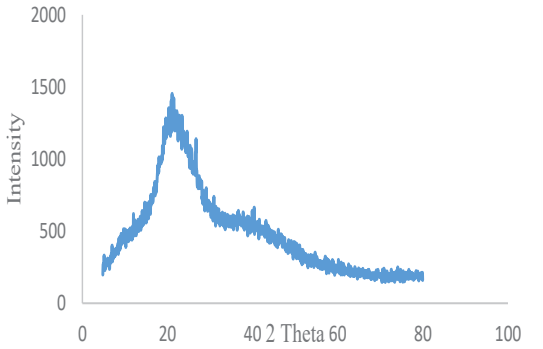

Fig. 2: X-ray diffraction pattern of nano-powdered synthetic bioactive glass of S646

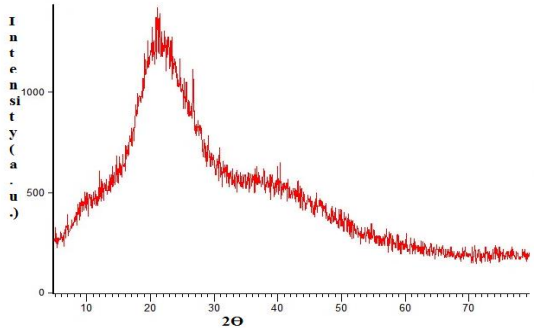

Fig. 3: X-ray diffraction pattern of chitosan /carbon nanotube composite.

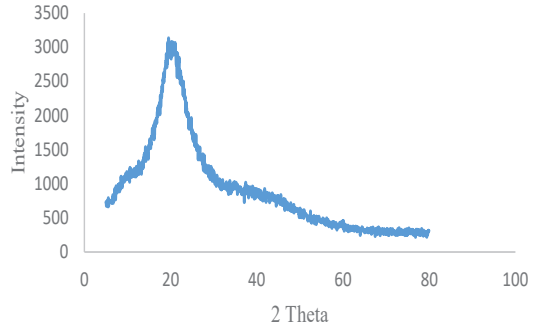

Fig. 4: X-ray diffraction pattern of S646 bio glass/ chitosan/CNT nanocomposite with 0.0045 bio glass

with a crystal structure. In the interpretation of the diffraction pattern, it could be presented that, this structure was well crystal lined.

The X-ray diffraction patterns of S646 bio glass/ chitosan/CNT nanocomposites are shown in Figs. 4-6.

As can be seen from the synthetic diffraction pattern of the synthesized nanocomposites, the synthetic nanosized particles are distinguishable from the synthesized composite dispersion pattern. The presence of glass in the material structure has led to the expansion of the diffraction pattern of the materials. Carbon nanotubes is involved in creating the crystal structure and the peak at approximately 10 degrees belong to chitosan. Table 2 shows the particle size values for the samples. By increasing the amount of bioactive glass from 0.0045 to 0.01 g, the peak intensity and particle size was decreased Owing to the presence of amorphous phase, crystallinity and crystal size were reduced.

Infrared spectroscopy analysis (FT-IR)

Fig. 7 shows Infrared spectroscopy analysis of bioactive glass of S646. The graph shows seven obvious bands, the bands at wavenumbers of 464 and 803 cm^{-1} are related to Si–O–Si bending vibrations and the band at 510 cm^{-1} is correlated to phosphate group ($PO4^{3-}$)[10].

The band at 1100 cm^{-1} was related to (PO) and, the band appeared at 966 cm^{-1} is related to SiO_2 stretching vibration [34]. The last band at 3452 cm^{-1} is assigned to O-H [9]. Fig. 8 shows the FT-IR spectrum of a chitosan / carbon nanotube composite sample. The peak with the wave number of 3353 cm^{-1} was related to the hydroxyl group of chitosan and the peak appeared at 1019 cm^{-1} was associated with the vibration of the C-O-C bond in chitosan. The peak with the wave number of 1400 cm^{-1} also indicated the vibration of the C-N bond in chitosan [11].

Structural changes at fluoride apatite-bioactive glass S646 nano-composite samples with different S646 bio glass percentages were investigated by FT-IR, which could be observed in Figs.9-11.

The peak at wave number of 900 $cm^{-1}$was related to *v*1 vibration and the peak at wave number of 464 $cm^{-1}$was related to *v*2 vibration and the wide peak at wave number of 1019 $cm^{-1}$was related to

Table 2: Comparison of particle size and crystallite percentage of composites.

Sample	Particle size	Crystallite percentage
S646 bio glass	48nm	86%
chitosan/CNT nanocomposite	47 nm	71%
S646 bio glass 0.0045/ chitosan/CNT nanocomposite	46 nm	67%
S646 bio glass0.0075/ chitosan/CNT nanocomposite	44nm	65%
S646 bio glass0.01/ chitosan/CNT nanocomposite	41nm	64%

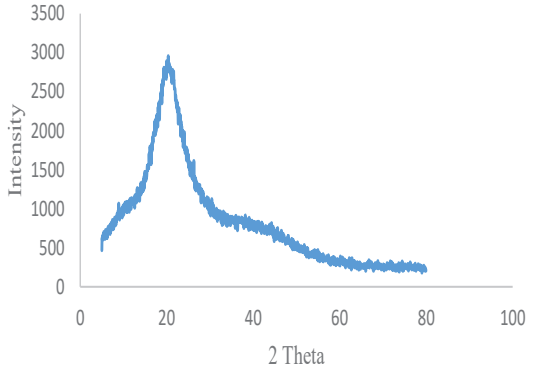

Fig. 5: X-ray diffraction pattern of S646 bio glass/ chitosan/CNT nanocomposite with 0.0075 bio glass

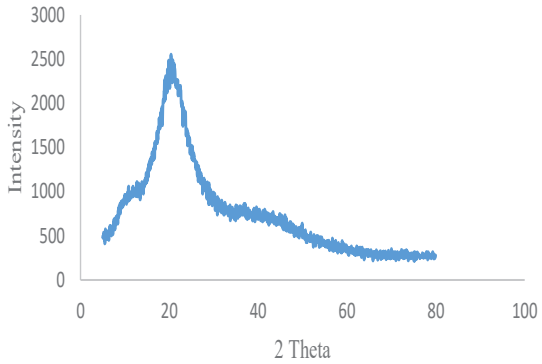

Fig. 6: X-ray diffraction pattern of S646 bio glass/ chitosan/CNT nanocomposite with 0.01 bio glass

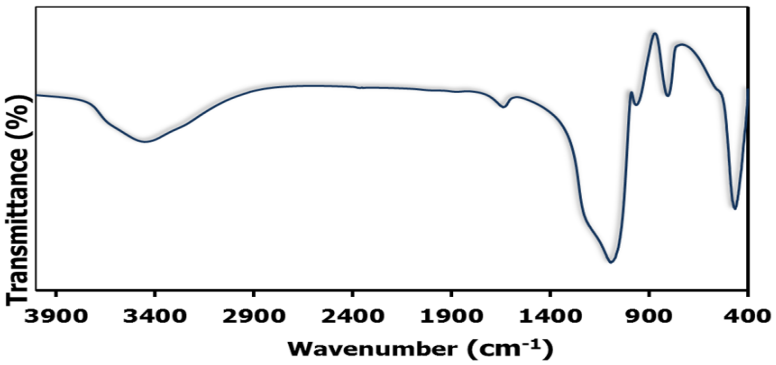

Fig. 7: Infrared spectroscopy analysis of bioactive glass of S646

C-O-C group in chitosan [1,11,35] .Finally, sharp peaks were located at 611 cm^{-1}, which belonged to the v4 vibration of PO_4^{3-} group. Additionally, with increasing the percentage of S646 bio glass phase, a strong and broad absorption band of the glass phase appeared at 980-1200 cm^{-1} which was related to the tensile vibrations of the Si-O-Si group and was gradually narrowed and focused to 987 cm^{-1} [10].The peak in the wave number of 1400 cm^{-1} also indicated the vibration of the C-N bond in chitosan [13, 36]. The peaks in the wave number of 3270-3350 cm^{-1} were related to the hydroxyl group of nanocomposites [35].

Morphological properties of nanopowders and nanocomposites by field emission scanning electron microscopy (FESEM)

Fig. 12a illustrated the FE-SEM images of synthesized S646 particles. It can be clearly demonstrated that, nanoparticles had spherical morphology with some agglomeration, which was due to the intrinsic nature of nanoparticles and their particle size ranges were from 40 to 25 nm. Scanning field emission microscopy images of the chitosan/ CNT in Fig. 12b shows the almost spherical structure of these synthesized particles with different particle sizes from about 49nm to 41nm.

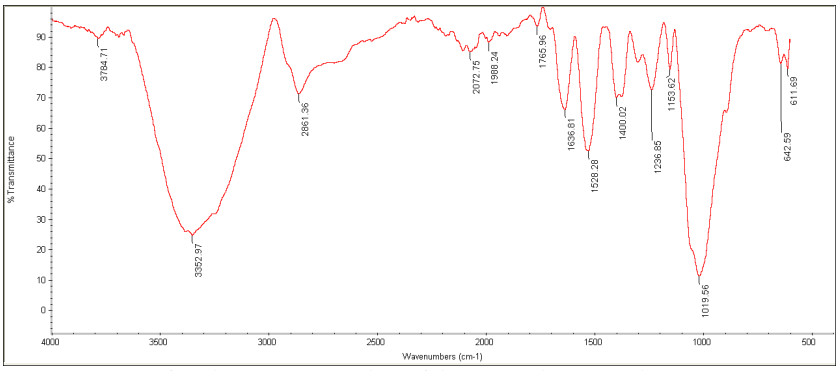

Fig. 8: Infrared spectroscopy analysis of chitosan /carbon nanotube composite

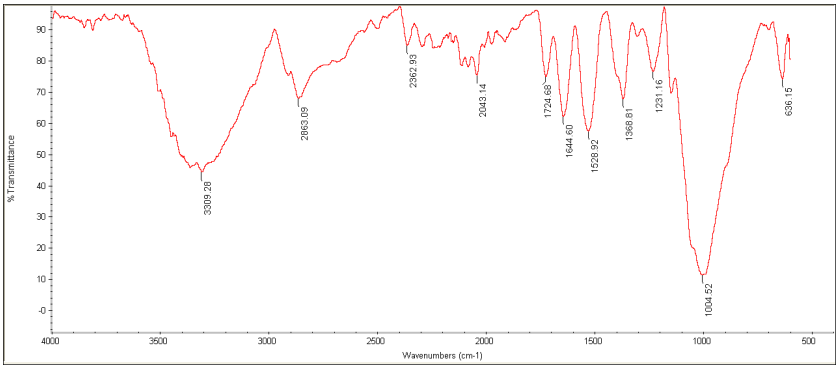

Fig. 9: Infrared spectroscopy analysis of S646 bio glass 0.0045/ chitosan/CNT nanocomposite

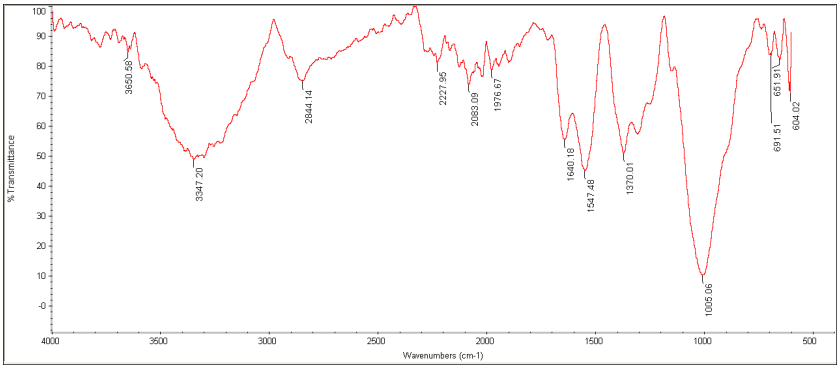

Fig. 10: Infrared spectroscopy analysis of S646 bio glass 0.0075/ chitosan/CNT nanocomposite

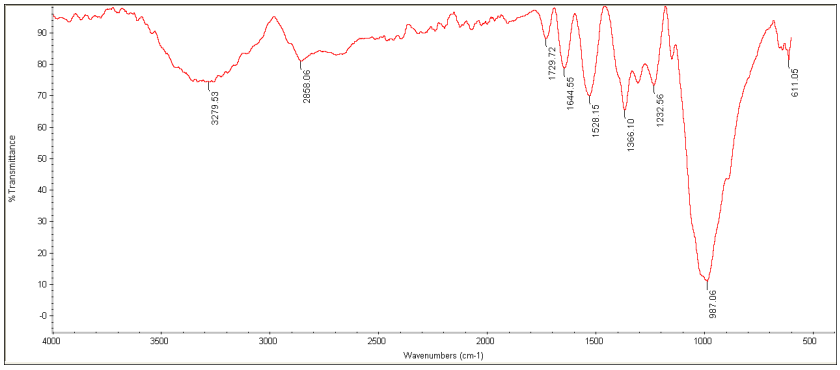

Fig. 11: Infrared spectroscopy analysis of S646 bio glass 0.01 chitosan/CNT nanocomposite

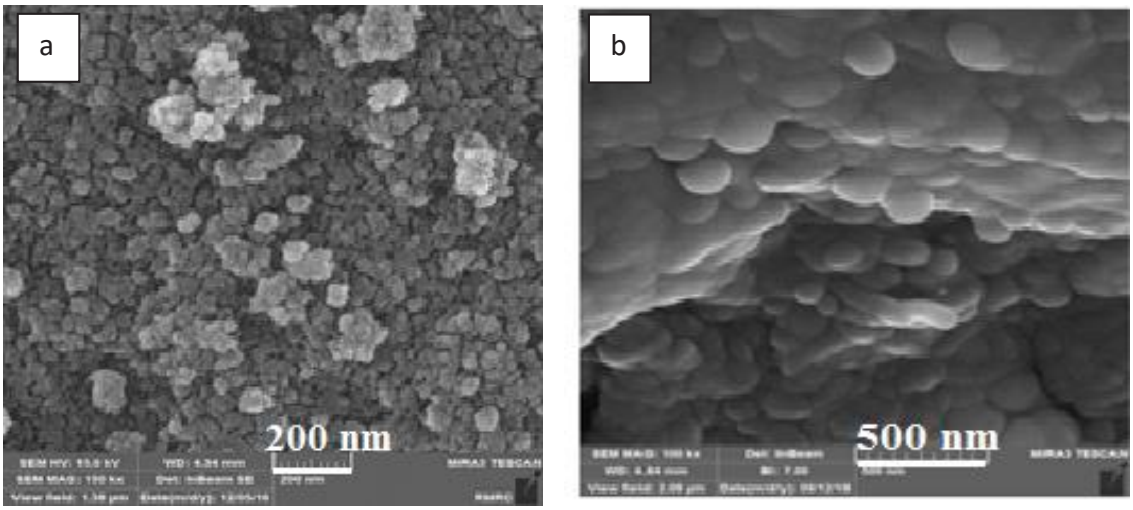

Fig. 12: Field emission scanning images of a) bioactive glass of S646, b chitosan/CNT nanocomposite.

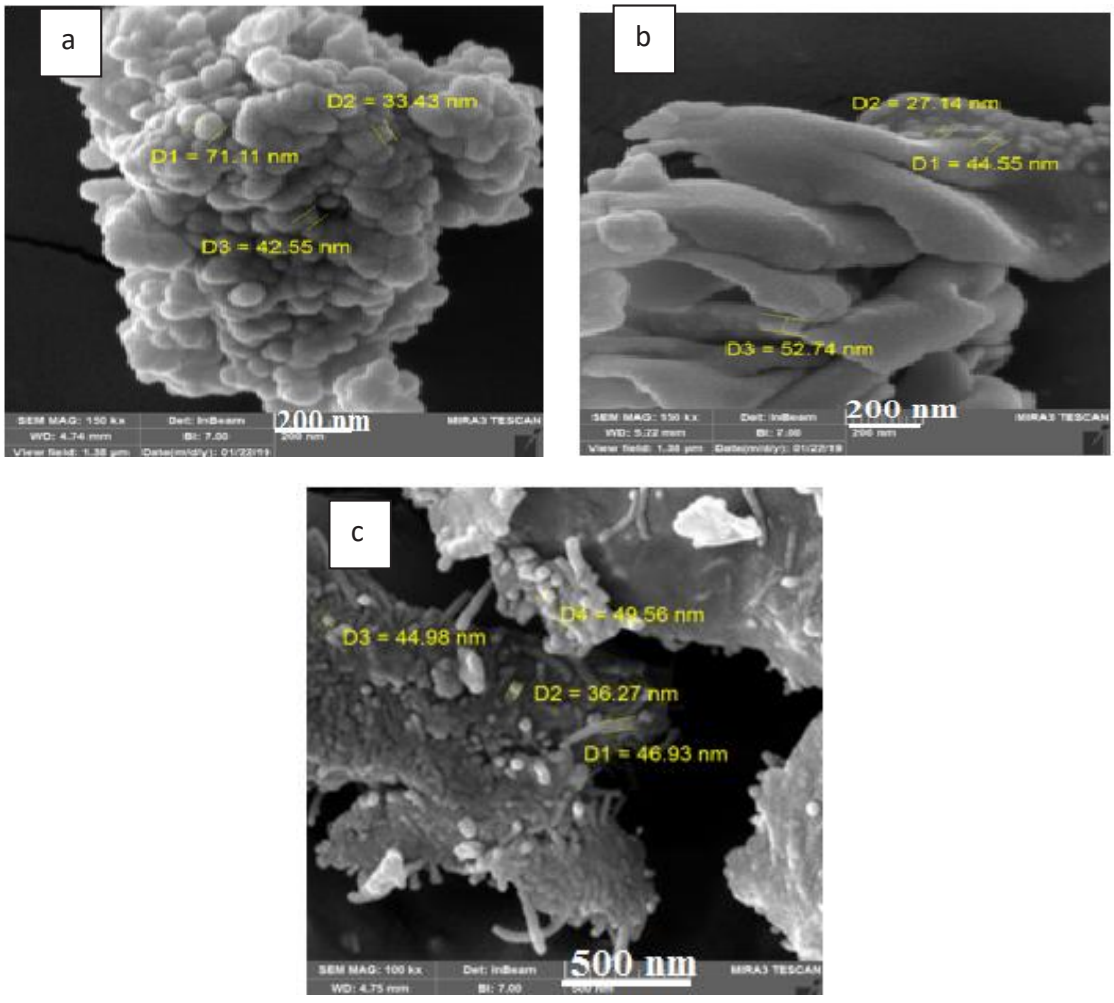

Fig. 13: Field emission scanning images of S646 bio glass / chitosan/CNT nanocomposites a)0.0045 g b)0.0075 g c)0.01 of S646 g bio active glass

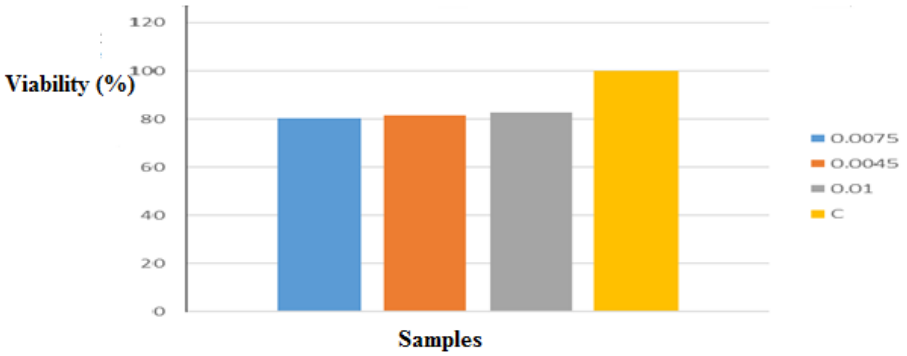

Fig. 14: MTT results of control sample and S646 bio glass / chitosan / CNT nanocomposites with different amounts of bio glass

Field emission scanning images of S646 bio glass / chitosan/CNT nanocomposites with different percentages of S646 bioactive glass are shown in Fig. 13. As it is shown the spherical shape of these synthesized particles have different particle sizes in three samples from about 41nm to 46nm, which confirmed the XRD results. Sample C with the highest amount of glass had the most complex morphology, which indicated the accumulation of glass particles with decreasing the amount of glass, the glass distribution and morphology, was changed. Therefore, the shape of the particles changed from a spherical state with the presence of glass in the composite and the particle size was reduced. By increasing the glass phase due to increasing the amorphous phase in the material, the crystallinity and the crystal size were reduced.

MTT Results

The results of the MTT test that were obtained after 3 days are presented in Fig. 14.

Regarding the shape, it can be seen that, by increasing the time of cell placement with the extract in all three main samples, the viability percentages was slightly increased from 80% to 82% by increasing the percentages of nano bioactive glass S646 from 0.0045 to 0.01 gr which could be evidence of increased cell growth in the presence of nanoparticles and nanocomposites and their lack of cytotoxicity. It also showed that S646 bio glass was a biocompatible material which promoted cell growth and proliferation and used as a scaffold for bone and has a beneficial effect on cell growth.

CONCLUSION

Nanobioactive glass S646 and S646 bio glass / chitosan/CNT nanocomposites has been prepared by modified sol-gel method. XRD results show a broad, shorter form that expressed the amorphous structure of the S646 bio glass nano powder synthesized and the crystalline phases of silicate (JCPDS 85033). Also, the crystallinity of the nano composites, decreased from 86% to 64%, by increasing the percentages of nanobioactive glass S646 from 0.0045 to 0.01 gr and the average diameter of the crystals increased from 41nm to 49 nm. Result of FT-IR analyses showed the purity in the structure of this nanoparticle and nano composite. The result of MTT assay indicated nontoxicity and with Increasing of the amount of S646 bio glass cell viability and scaffold biocompatibility was increased.

CONFLICT OF INTEREST

The authors declare that they have no conflict of interest.

STATEMENT

Ethical approval: This article does not contain any studies with human participants performed by any of the authors.

Ethical approval: This article does not contain any studies with animals performed by any of the authors.

Ethical approval: This article does not contain any studies with human participants or animals performed by any of the authors.

REFERENCES

[1] Baino F , Hamzehlou S , Kargozar S. Bioactive glasses: Where are we and where are we going. J. Funct. Biomater. 2018; 9:1-26. https://doi.org/10.3390/jfb9010025

[2] Fathi M H , Hanifi A l-gel method, Mater. Lett.2007; 61 : 3978-3983. https://doi.org/10.1016/j.matlet.2007.01.028.

[3] Hench L L , Jones R J. Bioactive materials for tissue engineering scaffolds, Biomedical Materials Research.2007; 28: 685-695. https://doi.org/10.1016/j.apsusc.2010.03.124

[4] Paluszkiewicz CA , Slosarczyk A , Pijocha D , Sitarz M ,

Bucko M M , Zima A. Synthesis, structural properties and thermal stability of Mn-doped hydroxyapatite. Journal of Molecular Structure.2010; 976:301-309. https://doi.org/10.1016/j.molstruc.2010.04.001

[5] Baino F , Novajra G , Brovarone C . Bioceramics and Scaffolds: A winning Combination for Tissue engineering. Frontiers in Bioengineering and Biotechnology.2015; 3:1-17.https://doi.org/10.3389/fbioe.2015.00202

[6] Khoshakhlagh P. Development and characterization of a bioglass/chitosan composite as an injectable bone substitute. Carbohyd Polym.2017; 157:1261-1271. https://doi.org/10.1016/j.carbpol.2016.11.003

[7] Shankhwar N, Srinivasan A. Influence of phosphate precursors on the structure, crystallization behaviour and bioactivity of sol-gel derived 45S5 bioglass. RSC AdvANCES.2015; l5:100762-100768. https://doi.org/10.1039/C5RA19184J

[8] Kokubo T. How useful is SBF in predicting in vivo bone bioactivity? Biomaterials.2007; 27:2907-2915. https://doi.org/10.1016/j.biomaterials.2006.01.017

[9] Jmal N , Bouaziz J . Synthesis, characterization and bioactivity of a calcium-phosphate glass-ceramics obtained by the sol-gel processing method. Mater Sci Eng C. 2017;71: 279-288. https://doi.org/10.1016/j.msec.2016.09.058

[10] Lindfors N. Bioactive glass S53P4 as bone graft substitute in treatment of osteomyelitis. Bone. 2010;47: 212-218. https://doi.org/10.1016/j.bone.2010.05.030

[11] Pishbin F,Simchi A, Ryan M P,Boccaccini A R.Surface & Coatings Technology Electrophoretic deposition of chitosan / 45S5 Bioglass ® composite coatings for orthopaedic applications. Surf. Coat. Technol.2011; 205:5260-8. https://doi.org/10.1016/j.surfcoat.2011.05.026

[12] Seo S , Kim J , Kim J , Lee J , Sang U, Lee E , Kim H. Enhanced mechanical properties and bone bioactivity of chitosan / silica membrane by functionalized-carbon nanotube incorporation. Compos. Sci. Technol. 2014;96: 31-7. https://doi.org/10.1016/j.compscitech.2014.03.004

[13] Jinshu M , Swapna K , Hai-Feng J , Michael J , Mc S. Study of the Near-Neutral pH-Sensitivity of Chitosan/Gelatin Hydrogels by Turbidimetry and Microcantilever Deflection. Biotechnology and Bioengineering.2020; 1-9.

[14] Diky M , Caroline W ,Heni R.. Encapsulation of Risperidone into Chitosan-based Nanocarrier via Ionic Binding Interaction. Procedia Chemistry.2014;13;92-100. https://doi.org/10.1016/j.proche.2014.12.011

[15] Liu XG. Preparation of Ibuprofen chitosan/montmorillonite microspheres by ionic cross-linking under microwave irradiation. Indian Journal of Chemical Technology (IJCT).2016;23:308-312.

[16] Vuong X , Mai Q , Tien Anh N , Hoa T , Investigation of Bioactive Glass-Ceramic 60SiO2-30CaO-10P2O5 Prepared by Hydrothermal Method. Advanced Dental Biomaterials and Therapeutic Substances.2019; 2019:1-9.

[17] Durgalakshmi D, Rakkesh R A , Balakumar S . Stacked bioglass/TiO2 nanocoatings on titanium substrate for enhanced osseointegration and its electrochemical corrosion studies Appl. Surf. Sci..2015; 349:561-9. https://doi.org/10.1016/j.apsusc.2015.04.142

[18]Pan L , Pei X , He R , Wan Q , Wang J. Colloids and Surfaces B : Biointerfaces Multiwall carbon nanotubes / polycaprolactone composites for bone tissue engineering application. Colloids Surfaces B Biointerfaces.2012; 93:226-34. https://doi.org/10.1016/j.colsurfb.2012.01.011

[19] P Newman,A Minett , R Ellis-Behnke, H Zreiqat. Carbon nanotubes: their potential and pitfalls for bone tissue regeneration and engineering, Nanomedicine: Nanotechnology. Biology and Medicine.2013;9:1139-1158. https://doi.org/10.1016/j.nano.2013.06.001

[20] Y Usui , K Aoki , N Narita , N Murakami , I Nakamura , K Nakamura , N Ishigaki , H Yamazaki , H Horiuchi , H Kato , S Taruta, Y A Kim , M Endo , N Saito. Carbon Nanotubes with High Bone-Tissue Compatibility and Bone-Formation Acceleration Effects. Smal.2008;4 :240-246. https://doi.org/10.1002/smll.200700670

[21] N O Chahine , N M Collette , C B Thomas , D C Genetos , G G Loots. Nanocomposite scaffold for chondrocyte growth and cartilage tissue engineering: effects of carbon nanotube surface functionalization. Tissue engineering. Part A.2014; 20:2305-2315. https://doi.org/10.1089/ten.tea.2013.0328

[22] F Mei , J Zhong , X Yang , X Ouyang , S Zhang , X Hu , Q Ma , J Lu , S Ryu , X Deng. Improved Biological Characteristics of Poly(l-Lactic Acid) Electrospun Membrane by Incorporation of Multiwalled Carbon Nanotubes/Hydroxyapatite Nanoparticles, Biomacromolecules.2007; 8:3729-3735. https://doi.org/10.1021/bm7006295

[23] A Abarrategi , M C Gutierrez , C Moreno-Vicente , M J Hortiguela , V Ramos, J L Lopez-Lacomba , M L Ferrer , F del Monte. Multiwall carbon nanotube scaffolds for tissue engineering purposes, Biomaterials.2008;29 :94-102. https://doi.org/10.1016/j.biomaterials.2007.09.021

[24] A R Boccaccini , F Chicatun , J Cho O. Bretcanu , J A Roether, S Novak , Q Z Chen. Carbon Nanotube Coatings on Bioglass-Based Tissue Engineering Scaffolds. Advanced Functional Materials.2007;17: 2815-2822. https://doi.org/10.1002/adfm.200600887

[24] E Hirata , M Uo , H Takita , T Akasaka , F Watari , A Yokoyama. Development of a 3D collagen scaffold coated with multiwalled carbon nanotubes. Journal of Biomedical Materials Research Part B: Applied Biomaterials.2009;90: 629-634. https://doi.org/10.1002/jbm.b.31327

[25] X Li , X Liu , J Huang , Y Fan , F-z Cui. Biomedical investigation of CNT based coatings, Surface and Coatings Technology.2011;206:759-766. https://doi.org/10.1016/j.surfcoat.2011.02.063

[26] J N Coleman , U Khan , W J Blau, Y K Gun'ko. Small but strong: A review of the mechanical properties of carbon nanotube-polymer composites. Carbon.2006;44:1624-1652. https://doi.org/10.1016/j.carbon.2006.02.038

[27] N Song , H Liu , Y Yuan , X Li , J Fang. Fabrication and Corrosion Resistance of SiC-coated Multi-walled Carbon Nanotubes. Journal of Materials Science & Technology.2013;29:1146-1150. https://doi.org/10.1016/j.jmst.2013.10.006

[28] K Hernadi , E Ljubović , J W Seo , L Forró. Synthesis of MWNT-based composite materials with inorganic coating. Acta Materialia.2003;51:1447-1452. https://doi.org/10.1016/S1359-6454(02)00539-6

[29] T Seeger, T Köhler , T Frauenheim , N Grobert , M Rühle , M Terrones , G Seifert. Nanotube composites: novel SiO2 coated carbon nanotubes. Chemical Communications. 2002; 34-35. https://doi.org/10.1039/b109441f

[30] T Lei , L Wang , C Ouyang , N.-F Li , L.-S Zhou. In Situ Preparation and Enhanced Mechanical Properties of Carbon Nanotube/Hydroxyapatite Composites. International

Journal of Applied Ceramic Technology.2011; 8 : 532-539. https://doi.org/10.1111/j.1744-7402.2010.02602.x

[31] P Khalid , M Hussain , P Rekha , A Arun. Synthesis and characterization of carbon nanotubes reinforced hydroxyapatite composite. Indian Journal of Science and Technology.2013; 6 : 5546-5551.

[32] R Sergi, D Bellucci , V Cannillo. A Review of Bioactive Glass/Natural Polymer Composites: State of the Art. Materials.2021;13:5560-5598.

[33] S Shrestha,B Kumar, S Sung W Ko, R Kandel, C H Park, C SangKim, Engineered cellular microenvironments from functionalized multiwalled carbon nanotubes integrating Zein/Chitosan @Polyurethane for bone cell regeneration. Carbohydrate Polymers.2021;251:117035-117045.

[34] L Zhao , L Gao. Novel in situ synthesis of MWNTs-hydroxyapatite composites. Carbon.2004;42:423-426. https://doi.org/10.1016/j.carbon.2003.10.024

[35] S Mukherjee , B Kundu , A Chanda , S Sen. Effect of functionalisation of CNT in the preparation of HAp-CNT biocomposites.Ceramics International.2015;41:3766-3774. https://doi.org/10.1016/j.ceramint.2014.11.052

[36] S Vahedi , R Mehdinavaz aghdam , A Rezayan , M Heydarzadeh Sohi. Carbon nanotubes reinforced electrospun chitosan nanocomposite coatng on anodized AZ31 magnesium alloy. Journal of Ultrafne Grained and Nanostructured Materials.2020;53:71-77.